ACS SyntheticBiology

Research Article

pubs.acs.org/synthbio

Visualization of Evolutionary Stability Dynamics and Competitive Fitness of *Escherichia coli* Engineered with Randomized Multigene Circuits

Sean C. Sleight* and Herbert M. Sauro*

University of Washington, Dept. of Bioengineering, Seattle, Washington 98195, United States

Supporting Information

ABSTRACT: Strain engineering for synthetic biology and metabolic engineering applications often requires the expression of foreign proteins that can reduce cellular fitness. In order to quantify and visualize the evolutionary stability dynamics in engineered populations of *Escherichia coli*, we constructed randomized CMY (cyan-magenta-yellow) genetic circuits with independently randomized promoters, ribosome binding sites, and transcriptional terminators that express cyan fluorescent protein (CFP), red fluorescent protein (RFP), and yellow fluorescent protein (YFP). Using a CMY color system allows for a spectrum of different colors to be produced under UV light since the relative ratio of fluorescent proteins vary between circuits, and this system can be used for the visualization of evolutionary stability dynamics. Evolutionary stability results from 192 evolved populations (24 CMY circuits with 8 replicates each) indicate that both the number of repeated sequences and overall expression levels contribute to circuit stability. The most evolutionarily robust circuit has no repeated parts, lower expression levels, and is about 3-fold more stable relative to a rationally designed circuit. Visualization results show that evolutionary dynamics are highly stochastic between replicate evolved populations and color changes over evolutionary time are consistent with quantitative data. We also measured the competitive fitness of different mutants in an evolved population and find that fitness is highest in mutants that express a lower number of genes (0 and 1 > 2 > 3). In addition, we find that individual circuits with expression levels below 10% of the maximum have significantly higher evolutionary stability, suggesting there may be a hypothetical "fitness threshold" that can be used for robust circuit design.

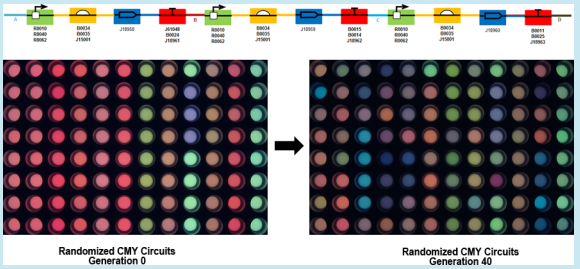

KEYWORDS: *synthetic biology, evolution, evolutionary stability, visualization, BioBricks, genetic circuits*

Engineering novel organisms for various synthetic biology[1−9] and metabolic engineering[10−16] applications first involves the design of a functional genetic circuit or metabolic pathway. This design process normally requires arranging genetic parts such as promoters, ribosome binding sites (RBSs), coding sequences, and transcriptional terminators in a particular order that is engineered and transformed into the host strain of interest. Although there are several software tools[17−22] now available to aid in design, it remains a daunting task that results in more failures than successes, and often requires part swapping and fine-tuning methods such as directed evolution to obtain the desired function.[23−26] Combinatorial methods can speed up the design-assembly-test engineering cycle by improving the odds that a circuit or pathway will function as desired and be robust to host context and environmental conditions.[21,27−31]

Another design consideration for circuits and pathways is evolutionary stability. It is well-known that new functions can impart a fitness cost[32−39] to organisms and that compensatory evolution can occur to ameliorate these costs.[36,37,40,41] With respect to synthetic biology, loss-of-function mutations can arise in synthetically encoded functions and nonfunctional organisms with higher fitness can outcompete functional ones over evolutionary time.[42−46] Genetic circuits can be rationally engineered to improve evolutionary stability by taking into consideration both expression levels that affect fitness and mutation rate, but most circuits will ultimately fail without a selective pressure to maintain their function.[45,46] For routine experiments, evolutionary stability may or may not be important, but for any application that requires growth over several generations (e.g., the production of biofuels in bioreactors), using evolutionary stability design considerations may help maximize the product of interest. As more complex circuits are engineered, evolutionary stability will become an increasingly important factor to consider during the design phase, and performing experiments to measure fitness and mutation rate before use of a circuit may become essential.

Experimental evolution[47] is a field that performs controlled experiments in the laboratory over evolutionary time scales to test hypotheses and study evolution in action. These experiments allow for the determination of genetic and phenotypic differences between evolved strains relative to their progenitors, and also whether replicate populations evolve in parallel or

Received: May 10, 2013
Published: August 16, 2013

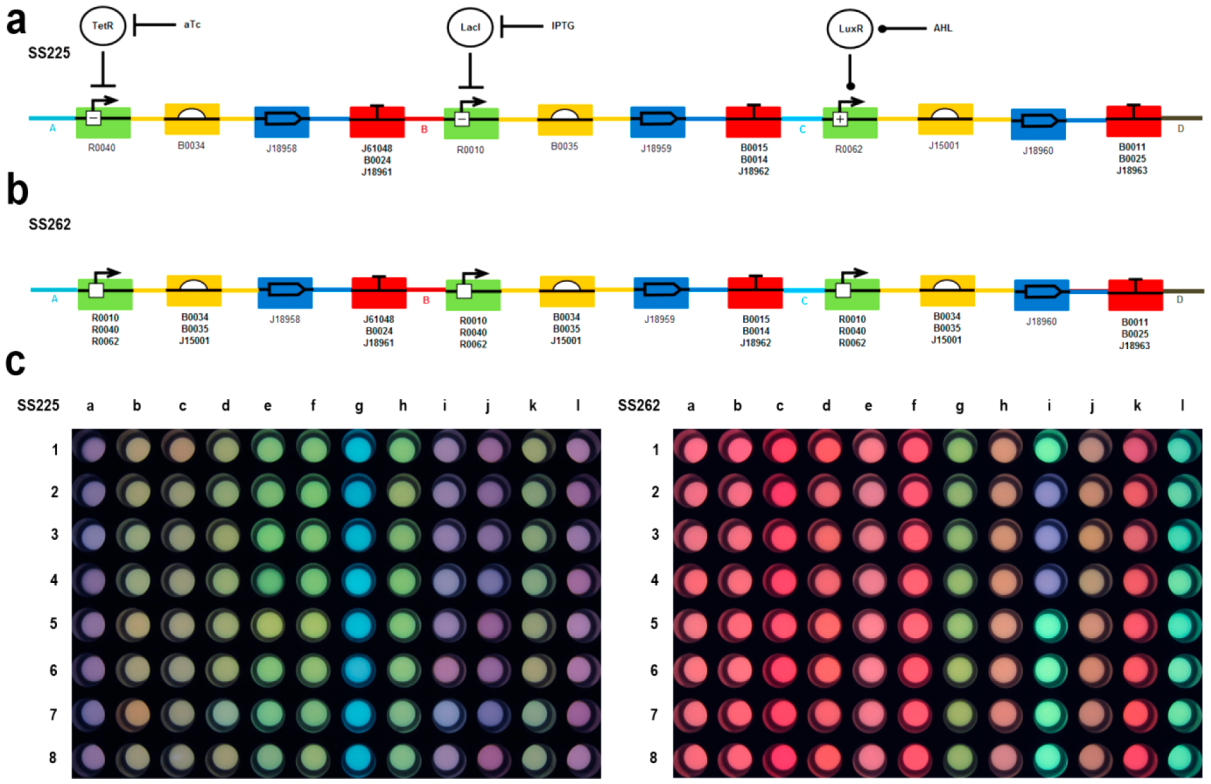

Figure 1. Randomized CMY circuits used in evolution experiments. (a) CMY circuits with randomized terminators (SS225). Circuits are shown with promoters (green box with regulation symbol and bent arrow), ribosome binding sites (orange box with half oval), fluorescent protein coding sequences (blue box with right-facing arrow), and transcriptional terminators (red "T" symbol). The regulation for each promoter is shown (see Methods), where regulation lines ending in a perpendicular line indicate inhibition and lines ending in a solid circle indicate activation. BioBrick part numbers (BBa_), PCR-amplified from Registry parts, are shown below each part symbol. Only the terminators were randomized in these circuits with parts shown underneath each terminator symbol (the sequencing results for each randomized circuit are shown in Supporting Information (SI) Figure 1). Nine of the twelve SS225 circuits are unique (SS225E = F = H, and SS225D = K). (b) CMY Circuits with randomized promoters, RBSs, and terminators (SS262). Circuits are shown with promoters, RBSs, and terminators randomized at each position (the sequencing results for each randomized circuit are shown in SI Figure 1). Eleven of the twelve SS262 circuits are unique (SS262A = B). (c) Visualization of *E. coli* expressing YFP, RFP, and CFP from SS225A–L circuits (left panel columns) and SS262A–L circuits (right panel columns) with eight replicates each (rows) in 96-well microtiter plates. See Methods and ref 66 for more details.

divergently.[48−54] The mutations identified in evolved strains can then be engineered into progenitor strains, or reversed, to measure their exact effect on fitness in a particular genetic context and environment.[52] Fitness is normally measured using direct competition experiments[49] between evolved and progenitor strains, or strains engineered with particular mutations, that have a marker to distinguish each competitor. Mutation rates can be measured using fluctuation tests or other experiments.[48,55−58]

Mutations that arise over the course of evolution are normally studied after a given number of generations have been carried out and natural selection has acted to fix certain mutations in the population. However, evolution is a dynamic process, and there are often several mutations with varying fitness effects competing with each other (known as clonal interference[59−62]), and as a result, certain beneficial mutations may be lost and other neutral or deleterious mutations may hitchhike to fixation along with other adaptive mutations.[47,48,54,63] For this reason, it becomes important to understand evolutionary dynamics through visualization in real-time. The VERT (Visualizing Evolution in Real-Time) system[60,61,64,65] is a tool used to identify fitter mutants that arise over evolutionary time scales and can enhance fitness landscape mapping of industrial relevant phenotypes. VERT typically works by labeling strains each with a different fluorescent protein that are seeded in a population to-be evolved, and as mutations arise in the evolved population, a labeled subpopulation with a particular beneficial mutation is expected to increase in proportion relative to other subpopulations.

In this study, we sought to visualize the evolutionary dynamics of *Escherichia coli* engineered with randomized 3-gene circuits that monocistronically express cyan fluorescent protein (CFP), red fluorescent protein (RFP), and yellow fluorescent protein (YFP) from independent promoters.[66] Since CFP, RFP, and YFP appear cyan, magenta, and yellow (CMY), respectively, under UV light, this allows for the visualization of color change over the course of an evolution experiment that can be verified with fluorescence measurements. It is currently unclear how three-gene circuits without selective pressure to maintain function will evolve over time with respect to (a) parallel or divergent evolution, (b) loss-of-function of 1 vs 2 vs 3 genes at a time, (c) repeated parts, and (d) relative expression levels.

During the course of evolution, the color of a particular population can change depending on how the relative fluorescent protein levels change over evolutionary time. For instance, based on the CMY color model, a CMY circuit that loses the Magenta function should in theory change from a complex color to green since only the Cyan and Yellow

dx.doi.org/10.1021/sb400055h | *ACS Synth. Biol.* 2013, 2, 519−528

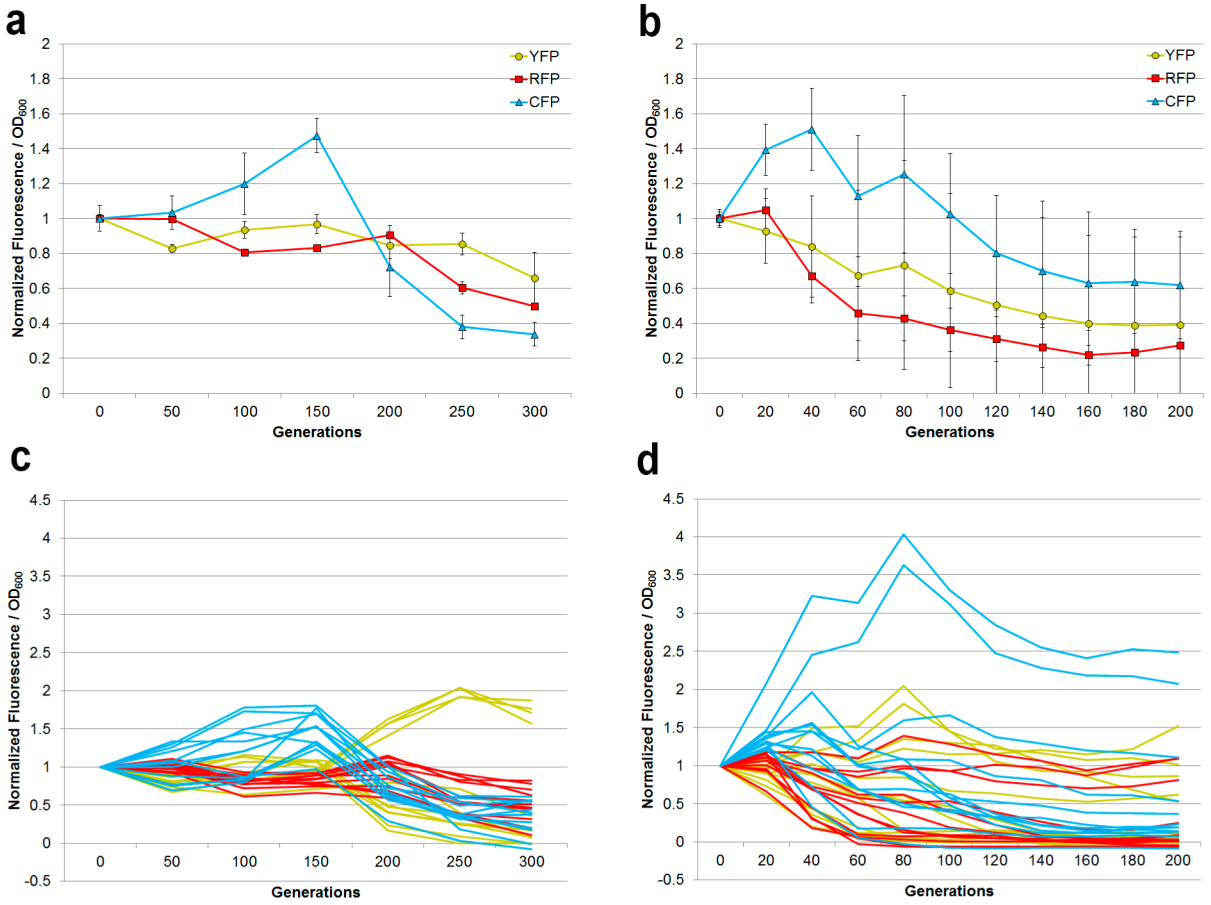

Figure 2. Evolutionary stability dynamics in randomized CMY circuits. The evolutionary stability dynamics of (a) SS225A–L circuits with randomized terminators and (b) SS262A–L circuits with randomized promoters, RBSs, and terminators. The mean normalized YFP, RFP, and CFP fluorescence for 12 circuits, each with eight replicate experiments, ± s.d, is plotted vs the number of generations. Individual evolutionary stability trajectories color-coded by fluorescent protein are plotted for (c) SS225A–L circuits and (d) SS262A–L circuits with eight replicate experiments each.

functions are expressed. The population color change then serves as an indicator of evolutionary stability and crude "mutational readout" of the genetic circuit. The color change can then be compared with quantitative data for each fluorescent protein and the loss-of-function mutations in evolved clones can be determined. The benefit of our CMY system for synthetic biology is that it allows us to visually identify evolved clones that have a particular color of interest, with the hope of finding circuit designs that are evolutionarily robust over a certain number of generations. Our system also allows us to visualize evolutionary dynamics in populations more easily, and mutant clones with unique colors can be used for direct competition experiments to measure fitness. The abilities of this CMY system thus allow us to better understand evolutionary stability dynamics and determine principles for designing industrially relevant robust synthetic systems.

RESULTS AND DISCUSSION

Engineering and Characterization of Randomized CMY Circuits. We previously studied the evolutionary stability and loss-of-function mutations in various 1 and 2-gene genetic circuits on high-copy plasmids.[45] In order to understand the evolutionary stability dynamics of more complex 3-gene circuits, we used medium-copy plasmids due to their increased stability (expressing three proteins from independent promoters on high-copy plasmids was generally found to be unstable). How predictable are evolutionary stability dynamics in more complex circuits, and what factors are important in determining their loss of function? Initially, we engineered a prototype circuit that produces cyan, magenta, and yellow (CMY) colors under normal light conditions to visualize evolution, but we found that certain aspects of this color system were not ideal, such as the use of X-gal in the media to visualize the expression of LacZ and use of a different molecule to obtain quantitative measurements.[67] Thus, another CMY circuit was engineered to visualize evolution under UV light, which produces more sensitive photographs compared to normal light conditions. This CMY circuit was rationally designed to not have repeated parts between individual YFP, RFP, and CFP expression cassettes, whereas randomized circuits may or may not have repeated parts. Due to combinatorial expression of YFP, RFP, and CFP from pTetR, pLacZYA, and pLuxR promoters a wide variety of colors can be seen between different circuits (Figure 1).

To generate a library of diverse circuits, two sets of randomized CMY circuits were engineered: 12 with the transcriptional terminators randomized (no repeated parts, Figure 1a and SI Figure 1a) and 12 with promoters, RBSs, and terminators randomized simultaneously that can generate circuits with repeated parts due to the same set of promoters and RBSs used at each position (Figure 1b and SI Figure 1b).[66] Of the 12 sequenced randomized terminator CMY circuits

dx.doi.org/10.1021/sb400055h | ACS Synth. Biol. 2013, 2, 519–528

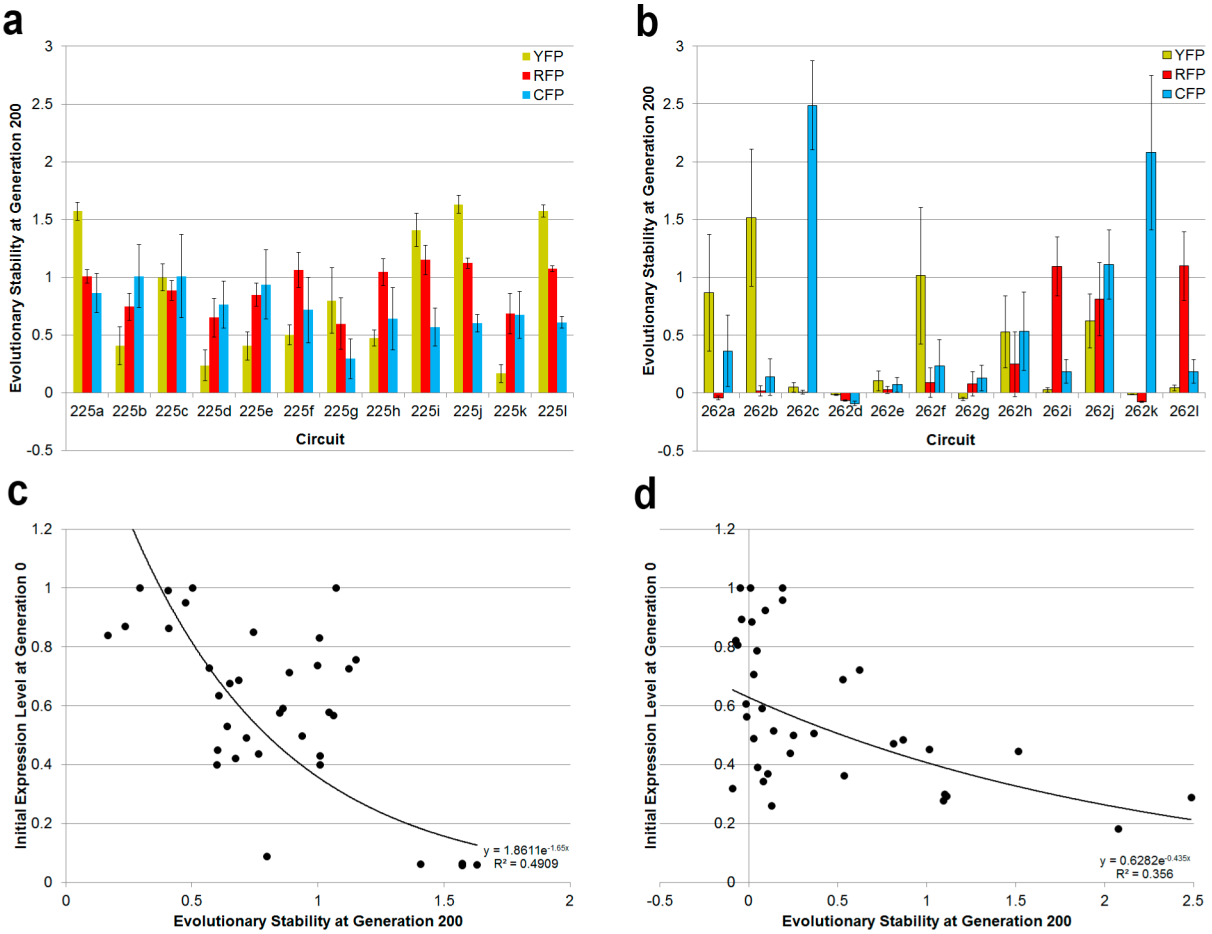

Figure 3. Evolutionary stability of randomized circuits vs rationally designed circuit (SS225D/K) at generation 200. The normalized YFP, RFP, and CFP fluorescence at generation 200 is plotted for (a) SS225A–L circuits and (b) SS262A–L circuits. The height of each bar represents the mean of eight experiments ± s.d. In order to understand the relationship between expression level and evolutionary stability, the relative normalized YFP, RFP, and CFP fluorescence at generation 0 relative to the mean is plotted vs the normalized fluorescence at generation 200 for (c) SS225A–L circuits and (d) SS262A–L circuits. Each data point represents the mean of eight experiments. The exponential fit equation and R^2 value is shown. See the main text for details.

(strain IDs SS225A-L), 9/12 are distinct, and of the 12 sequenced randomized promoter-RBS-terminator CMY circuits (strain IDs SS262A-L), 11/12 are distinct. In order to have additional biological replicates for evolution experiments, all 24 circuits were used, despite only 20 circuits being unique. See ref 66 for details on the construction of these circuits. Although each fluorescent protein can be independently and combinatorially expressed, the relative expression level of a particular fluorescent protein is affected when multiple fluorescent proteins are expressed (e.g., CFP expression decreases when other inducers besides AHL are added simultaneously) (SI Figures 2 and 3). In general, the expression of a particular fluorescent protein decreases with the number of additional fluorescent proteins being produced at the same time. This same observation of nonindependent expression was also found in the prototype CMY circuit that expresses GFP, RFP, and LacZ.[67] Presumably, there is competition for transcriptional and translational machinery when multiple transcripts are produced simultaneously from multiple copies of plasmid DNA. Nonetheless, SI Figure 3 shows that distinct colors are produced from various circuits for each unique combination of inducers.

To visualize the color in these randomized circuits, we performed experiments using three inducers to turn all three colors on and can see that different colors are generated due to the relative proportions of each fluorescent protein (Figure 1c, Methods). The various colors highlight the variation that can be produced using various combinations of parts. While there is some variation in SS225 circuits due having different terminators, there is more variation seen in SS262 circuits due to having all parts besides the coding sequence randomized. Since the evolutionary stability dynamics were found to be nearly identical between replicate evolved populations of a single clone,[67] we picked eight clones for each randomized circuit to perform evolution experiments. Although the color is generally similar between clones of a particular randomized circuit, there are certain clones with color differences due to YFP loss-of-function that changes the population to a purpleish color due to expression of RFP and CFP (e.g., SS262I). The variation in SS225 clones is primarily due to having a particular terminator (J18961) that decreases the relative steady-state YFP expression and evidently causes read-through transcription into the RFP portion of the circuit since relative steady-state RFP expression is increased. The blush pink color of many of these circuits is evidently due to the high expression of RFP from the strong pLuxR promoter that overpowers the other primary colors.

dx.doi.org/10.1021/sb400055h | ACS Synth. Biol. 2013, 2, 519–528

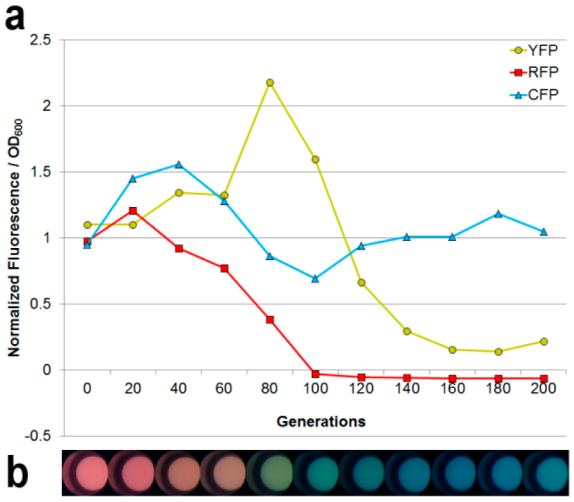

Generation	YFP	RFP	CFP	Color	Mutation
0	+	+	+	Pink	None
30	+	-	+	Green	Deletion between repeated R0062 promoters
90	+	-	-	Yellow	Deletion of *luxR* on vector
150	-	-	+	Cyan	Deletion that produces CFP with positions 1-54 YFP and 67-729 CFP
200	-	-	-	None	Deletion between suffix and terminator on vector

Figure 4. Evolutionary stability dynamics, phenotypes, and genotypes of an evolved population. (a) The evolutionary stability dynamics of the SS262A-5 population. Normalized fluorescence of YFP (J18958), RFP (J18959), and CFP (J18960) is plotted vs the number of generations for a single experiment. (b) Visualization of the SS262A-5 population every 20 generations in a 96-well plate for over 200 generations. Each well is placed below the generation time point in the evolutionary stability graph above. (c) The mutant phenotypes and mutations of the SS262A-5 population at different generation time points. The YFP, RFP, and CFP phenotypes (+ indicates expression above background levels and − indicates expression at background levels) of the ancestral circuit at generation 0 and mutants at generations 30, 90, 150, and 200 are shown. (d) The mutant genotypes (circuit diagrams) of the SS262A-5 population at different generation time points. Parts that are expressed in the reverse direction on the vector are shown (see Methods and ref 66. See main text for details and Table 1 for fitness measurements.

Evolution Experiments on Randomized CMY Circuits. We performed evolution experiments on these 24 randomized circuits (SS225A-L and SS262A-L) to measure and visualize their evolutionary stability dynamics and determine which designs were the most evolutionarily robust (Figure 2). The mean YFP, RFP, and CFP expression levels in SS225 terminator-randomized circuits are relatively stable (about 75% of the maximum) through the 200 generation time point but fall to about 50% after 300 generations (Figure 2a). The SS262 promoter-RBS-terminator randomized circuits have an evolutionary half-life of about 120 generations, and the mean expression decreases to about 35% of the maximum after 200 generations (Figure 2b). Since each randomized circuit set (SS225 and SS262) hase different antibiotic resistance markers, direct comparisons between these sets should be made with caution. The decreased evolutionary stability in SS262 circuits may be due to (1) having about a 20% higher expression level on average relative to SS225 circuits, (2) having repeated promoter and RBS parts that can cause deletions between repeated sequences[44−46] (SI Table 1), or (3) having chloramphenicol resistance instead of kanamycin resistance in SS225. We evolved the SS225 circuits for 300 generations (100 generations longer than for SS262 circuits) until the mean YFP, RFP, and CFP expression levels reached about 50% to determine what circuit had the highest evolutionary stability. Relative to a rationally designed circuit (SS225D/K), one circuit (SS225A) had about 3-fold increased evolutionary stability in all three fluorescent proteins and 6-fold greater stability if all three are averaged on a scale from zero to one (SI Figure 4). Interestingly, the four most evolutionarily robust circuits all had same terminator (J18961) that is inefficient as a terminator by itself, but improves evolutionary stability of both YFP and RFP, likely because it decreases steady-state YFP expression levels.

The variation in individual evolutionary stability trajectories for YFP, RFP, and CFP is much higher in SS262 circuits relative to SS225 circuits (Figure 2c and d). Certain trajectories increase higher than their initial value, presumably due to the balancing of expression levels either due to physiological adaptation or loss-of-function mutations. The evolutionary stability dynamics of each individual randomized CMY circuit are shown in SI Figures 5 and 6. We also visualized the evolutionary stability dynamics of the SS225 and SS262 circuits by producing movies from photographs of the populations that were concentrated and imaged under UV light at particular evolutionary time points (SI Figure 7, SI Videos 1 and 2). Relative to SS225 populations, SS262 populations have more dynamic color changes over evolutionary time and between replicate populations, in agreement with the quantitative measurements.

To analyze the results of these evolution experiments at the generation 200 time point, the mean and individual YFP, RFP, and CFP expression levels were plotted for SS225 and SS262 circuits (Figure 3). The SS225 circuits express either 2 or 3 fluorescent proteins on average, whereas the SS262 with more repeated parts express either 0, 1, or 2 (Figure 3a and b). This result makes sense when looking at the individual parts for each circuit since there are more opportunities for deletions between repeated parts in SS262 circuits that will remove two functions simultaneously. When the individual YFP, RFP, and CFP expression levels at the generation 200 time point are plotted against the initial expression level, there is a moderate trend for stability to decrease with increasing expression levels (Figure 3c and d), in agreement with previous results using 1 and 2 gene circuits.[45] The SS225 circuits may have a stronger relationship between evolutionary stability and initial expression levels (R^2 = 0.491 vs 0.356), probably due to having less part variation and a lower number of repeated sequences (SI Table 1). It is interesting to note that the four data points in the lower right corner of the graph all have below 10% expression relative to the highest expressing circuit. To determine if there is a possible "fitness threshold" for synthetic circuits, we grouped the evolutionary stability for the five data points that were below the 10% expression threshold and compared them to the

dx.doi.org/10.1021/sb400055h | ACS Synth. Biol. 2013, 2, 519−528

stability values for the other 31 data points above the threshold. The highly significant p-value of 0.001 (two-tailed *t*-test, unequal variances) suggests that there may be a hypothetical expression threshold (proxy for a fitness threshold) that can be used to maximize the lifespan of multigene circuits. In other words, perhaps the evolutionary stability of more complex circuits can be maximized if the circuit or pathway is designed to express each protein (or RNA) below a hypothetical fitness threshold.

The most evolutionarily robust randomized circuits (SS225A and SS225C) are both over 95% stable after 200 generations, based on the mean YFP-RFP-CFP expression levels. To better understand what part combinations make the most robust circuits, we plotted the evolutionary stability vs the initial expression level for all 24 randomized circuits and see that there is a moderate trend (R^2 = 0.361) (SI Figure 8a). This relationship is not as strong as that measured for 1 and 2 gene circuits (R^2 = 0.597[45]) and may indicate that mutation rate is more of a factor in determining the evolutionary stability in more complex circuits. Next, the evolutionary stability was plotted against the number of repeated sequences, and there is also a moderate trend (R^2 = 0.394) (SI Figure 8b). However, when both initial expression and number of repeated sequences are plotted together as a function vs evolutionary stability, there is a stronger trend (R^2 = 0.497) than both individually (SI Figure 8c, Methods). The two most robust circuits (SS225A and SS225C) are in the upper left quadrant of this graph, likely due to having both low expression levels and number of repeated sequences (SI Figure 8c, SI Table 1). These results indicate that, to maximize evolutionary stability, there should be design considerations with respect to both expression level and repeated sequences. Also, since only about half of the variability in evolutionary stability could be explained by two factors (initial expression level, as a proxy to fitness, and the number of repeated sequences, as a proxy to mutation rate), other factors such as repeat length, distance between repeats, and factors that measure cellular physiology and toxicity are needed to fully explain the evolutionary stability of genetic circuits.

Competitive Fitness between the Ancestor and Mutants in an Evolved Population. Next, in order to better understand the relationship between fitness and evolutionary stability in CMY circuits, we selected one population to study in further detail called SS262A-5 (Figure 4). This population was chosen because the color change over evolutionary time was dynamic and changed from a blush pink color to green to cyan over 200 generations (Figure 4a and b). The quantitative evolutionary stability data shows that RFP is lost in the population first, then YFP, and CFP remains stable after 200 generations (Figure 4a, see SI Figure 9 for the relative proportions of each fluorescent protein at different evolutionary time points). The color change in this population over time matches the evolutionary stability data well, since the population turns green as RFP is lost in the population, then turns cyan as YFP is lost in the population, as expected using a CMY color model (Figure 4b). Three clones were chosen from evolutionary time points at generations 0, 30, 90, 150, and 200 with particular phenotypes that express different combinations of fluorescent proteins (Figure 4c). These clones were then sequenced to determine the genotypes of each mutant (Figure 4d). All three clones at the generation 30 time point have a deletion between repeated R0062 promoters that effectively deletes out the RFP expression cassette. The generation 90 time point clones all have no mutations in the CMY circuit relative to generation 0, but have the same deletion on the vector that inactivates the expression of LuxR, controlling RFP and CFP expression. Generation 150 clones all have a deletion between repeated sequences on YFP and CFP that interestingly produce a new hybrid fluorescent protein that maintains CFP expression but not YFP expression. Finally, three rare nonfunctional clones at the generation 200 time point all have the same deletion between the suffix and a terminator on the vector that removes the entire CMY circuit.

To understand the fitness differences between the SS262A-5 mutants vs the ancestor, we performed direct competition experiments between clones (see Methods for details). Competition experiments allow for exact differences in fitness to be measured between an evolved clone and its ancestor in a particular environment.[47] Normally, relative fitness is measured by competing the ancestral and evolved clones in the same environment as that used for the evolution experiment. The two competitors are first grown separately to make sure they are acclimated to the competition environment; then, they are mixed at equal volumetric ratios and grown together in the competition environment. Both competitors need to have a marker that distinguishes them so that the cell density can be measured at the initial time point (t = 0) and after the competition (t = 1). Relative fitness is then calculated based on the ratio of the growth rates between evolved and ancestral clones.

In the context of synthetic biology, because the ancestral and evolved clones have distinct colors under UV light, they can be distinguished easily and thus directly competed (Figure 4c, SI Figure 10). As a control measure, we independently propagated each clone in the same competitive environment and observed that the color did not change over the course of the experiment (this would give misleading fitness measurements if so) (SI Figure 10). Initially, we competed the ancestor (generation 0) against each of the evolved clones at generations 30, 90, 150, and 200 separately and observed that for the latter three generation time points, the mutants outcompeted the ancestor so quickly that there were no ancestral colonies on the t = 1 plates, and hence no fitness data. Therefore, we performed competition experiments to compete generation 0 vs 30, 30 vs 90, 90 vs 150, and 150 vs 200 so that both competitors were more equally matched (Table 1). The results show that the generation 30 clone has about an 89% improvement in fitness relative to the ancestor, the generation 90 clone has about a 57% fitness improvement over generation 30, and the generation 90, 150, and 200 clones that express zero or one genes have relatively equal fitness that is not statistically different. The large fitness differences are likely due to plasmid DNA loss-of-function mutations but could also partly be due to

Table 1. Fitness Differences between Mutants in the SS262A-5 Population[a]

competition	relative fitness	standard deviation
Gen 30/Gen 0	1.887	0.029
Gen 90/Gen 30	1.574	0.087
Gen 150/Gen 90	0.993	0.011
Gen 200/Gen 150	0.960	0.039

[a]For each competition experiment with two competitors for a particular generation timepoint (Gen 0, 30, 90, 150, 200), the relative fitness and standard deviation is shown for three replicate experiments. See Methods for details.

dx.doi.org/10.1021/sb400055h | ACS Synth. Biol. 2013, 2, 519−528

unknown mutations on the chromosome, and the exact fitness effects of plasmid mutations could be experimentally tested by retransforming these mutant plasmids into the background strain. It is unknown whether the loss-of-function mutations in this population occurred sequentially, or independently. Certainly generation 30 and 90 clones have distinct mutations that occurred independently, but generation 30 and 150 clones could have occurred sequentially or not.

Overall Conclusions and Future Directions. Overall, these evolutionary stability and competitive fitness results demonstrate that synthetic functions can impart a large fitness disadvantage to cells and evolutionary adaptation occurs in order to relieve the metabolic load or toxicity associated with expressing foreign proteins. Medium-copy plasmids were used in this study for visualization purposes, but evolutionary stability certainly would have been improved using low-copy plasmids or circuits integrated into the chromosome. We find that evolutionary stability dynamics are highly stochastic between replicate evolved populations with the same exact circuit and even more stochastic between different circuits due to the variation in parts used. In general, circuits with high evolutionary stability have both low expression levels and a low number of repeated sequences—this result indicates that both fitness and mutation rate should be considered when designing circuits, in addition the careful selection of choice parts. Randomization methods should be used in order to maximize the chances of identifying circuits that have high evolutionary stability when a large number of generations are required for study or applied use.

Specific software tools that include design specification rules for grammar[19,22] could be used in the future to check for repeated parts and sequences to maximize evolutionary stability. Software tools that take into account predicted expression levels using particular promoters and RBSs[8,9] may also be useful for improving the predicted evolutionary stability of a circuit or metabolic pathway. A suggested approach for metabolic engineering would be to first identify pathway configurations that have tolerable productivities/titers, then optimize the pathway to not use repeat parts and reduce expression levels without compromising productivity. It would be very useful to have a quantitative gauge between the economic trade-offs between reducing enzyme expression and decreased evolutionary stability risks.

In general, for future studies, more work is needed to (1) develop more experimental tools or strategies for maximizing evolutionary stability,[46] (2) identify more creative linkages between fitness and synthetic functions to take advantage of evolutionary engineering,[68,69] (3) calculate whether a hypothetical "fitness threshold" for synthetic functions exists to determine the metabolic burden a particular strain can handle before evolutionary stability becomes a problem, or whether this burden is always dependent on the foreign RNA or proteins being expressed, and (4) develop a more thorough understanding of the exact variables that contribute to evolutionary stability that will someday allow software to design robust synthetic systems for us.

METHODS

Parts, Vectors, and Plasmid Engineering. All standard biological parts (BioBricks) were obtained from the Registry of Standard Biological Parts (partsregistry.org) except for select parts obtained from DNA2.0 (J18961, J18962, and J18963 terminators), the Klavins Lab (maxRFP coding sequence, equivalent to the E1010 Monomeric Red Fluorescent Protein, except that the first few codons were re-engineered to increase expression levels), or the Elowitz Lab (eYFP and eCFP coding sequences). All parts and vectors used in this study are described in SI Table 2, and all strains produced using the Randomized BioBrick Assembly method are described in SI Table 3 and ref 66.

Genetic Circuit Characterization. *CMY Color Visualization and Inducer Experiments.* The R0010 (pLacZYA with CAP binding site, regulated by LacI), R0040 (pTetR), and R0062 (pLuxR) promoters can be induced by Isopropyl-β-D-thiogalactopyranoside (IPTG), Anhydrotetracycline (aTc), and 3-oxohexanoyl-homoserine lactone (AHL), respectively. Media was prepared in an Eppendorf deep 96-well plate with 1.5 mL LB + 50 μg/mL kanamycin or 34 μg/mL chloramphenicol, 100 μM IPTG, 100 nM AHL, and 1 ug/mL aTc (for full induction). Plasmids with randomized CMY circuits[66] were transformed into MG1655 Z1,[28,45,46,67] which constitutively overexpresses LacI and TetR from the chromosome. Eight transformant colonies of each randomized CMY circuit were grown in LB and appropriate antibiotics at 37 °C shaking at 250 rpm overnight, then saved for long-term storage at −80 °C in 15% glycerol. Circuits were characterized by first streaking out freezer stocks on LB agar plates with appropriate antibiotics (50 μg/mL kanamycin or 34 μg/mL chloramphenicol) and incubation at 37 °C overnight, then colonies were grown for 24 h in 1.5 mL LB + 50 μg/mL kanamycin or 34 μg/mL chloramphenicol at 37 °C shaking at 250 rpm in an Eppendorf deep 96-well plate sealed with a Thermo Scientific gas permeable membrane for maximum oxygen diffusion. The cultures were then diluted 1:1000 into 1.5 mL LB + 50 μg/mL kanamycin or 34 μg/mL chloramphenicol, with and without inducers (100 μM IPTG, 100 nM AHL, and 1 ug/mL aTc), and grown at 37 °C shaking at 250 rpm for 24 h, then steady-state fluorescence and OD_{600} was measured. To calculate the induced/uninduced ratio (a metric to measure circuit on−off behavior), induced and uninduced fluorescence readings are first divided by OD_{600} to normalize for cell density, then the induced fluorescence/OD_{600} value is divided by uninduced fluorescence/OD_{600} value for each replicate. For color visualization, the cultures were centrifuged at 2500 rpm for 10 min at 4 °C, the supernatant was removed, then the cells were washed with 500 μL of water, centrifuged again at 2500 rpm for 10 min at 4 °C, the supernatant was again removed, then the cells were resuspended in 100 μL of water and transferred into a black, clear-bottom 96-well microplate (Costar). The plate was incubated for an additional 24 h at room temperature, then visualized with a UV transilluminator (Fotodyne, 312 nm wavelength, low intensity) attached to a Fotodyne Apprentice System equipped with a color digital camera (after removal of the UV filter).

Evolution Experiments. Eight colonies for each of the Z1 strains transformed with randomized CMY circuit plasmids (SS225A-L and SS262A-L)[66] were grown in 1.5 mL LB + 50 μg/mL kanamycin or 34 μg/mL chloramphenicol, 100 μM IPTG, 100 nM AHL, and 1 ug/mL aTc in an Eppendorf deep 96-well plate sealed with a Thermo Scientific gas permeable membrane. These cultures were grown at 37 °C shaking at 250 rpm and propagated every 24 h by using a 1:1000 dilution to achieve about 10 generations per day ($\log_2 1000 = 9.97$). Every 24 h, cell density (OD_{600}) and fluorescence of evolved populations were measured. The 24 h measurement time point was chosen because the rate of change of fluorescent

dx.doi.org/10.1021/sb400055h | ACS Synth. Biol. 2013, 2, 519−528

protein expression is close to steady-state. Fluorescence for each color was then divided by OD_{600} to calculate the expression normalized for cell density (Normalized Fluorescence/OD_{600}). To calculate the relative normalized fluorescence, values were divided by the highest normalized fluorescence/OD_{600} value for a particular group.

Notes on the 24 h Growth Cycle. Over the 24 h growth cycle used for evolution experiments, the cells spend 8−12 h in lag/growth phase and the remaining time in stationary phase. The number of generations that take place during evolution experiments is set by the dilution rate, not the growth rate, as it is expected that some strains grow more slowly than others. Therefore, as long as the cells have finished growing by the 24 h time point, there will theoretically be about 10 generations per day achieved for all strains. Evolutionary stability dynamics may be different when cells are propagated under continuous culture where cells are always in growth phase vs growth phase + stationary phase.

Visualizing Cell Color in Evolved Populations and Clones. The cell color for populations or clones was visualized by centrifuging 1.5 mL cultures in a Sorvall Legend 23R centrifuge at 2500 rpm for 10 min at 4 °C, removing the supernatant, washing with 500 μL of water, centrifuging again at 2500 rpm for 10 min at 4 °C, removing the supernatant, then resuspending the cells in 100 μL of water in a black, clear-bottom 96-well plate (Costar). Cells incubated for 24 h at room temperature to allow for stronger color development before photographing the plates with a UV transilluminator (Fotodyne, 312 nm wavelength, low intensity) attached to a Fotodyne Apprentice System equipped with a color digital camera (after removal of the UV filter).

Sequencing Plasmids in Evolved Clones. Populations at appropriate evolutionary time points were streaked out on LB + 50 μg/mL kanamycin or 34 μg/mL chloramphenicol agar plates, supplemented with inducers (100 μM IPTG, 100 nM AHL, and 1 ug/mL aTc). A single clone or multiple clones from each population were grown in 8 mL LB + 50 μg/mL kanamycin or 34 μg/mL chloramphenicol for 24 h at 37 °C shaking at 250 rpm. Plasmids were extracted using the Qiagen Miniprep Kit and submitted to the Genewiz or UW HTseq (www.htseq.org) sequencing facility for sequencing. Purified plasmid DNA was sequenced using VF2/VR primers specific to the pSB3K3 vector (about 100 bp on either side of the circuit) and internal primers specific to the circuit.

Direct Competition Experiments to Measure Fitness. Relative fitness was measured by individually growing each competitor strain in 5 mL of LB media with 34 μg/mL chloramphenicol at 37 °C shaking at 250 rpm for 24 h. Competitors were then mixed at a 1:1 volumetric ratio by diluting each 1:1000 into 1.5 mL LB + 34 μg/mL chloramphenicol, 100 μM IPTG, 100 nM AHL, and 1 μg/mL aTc, with three replicates each, in an Eppendorf deep 96-well plate sealed with a Thermo Scientific gas permeable membrane. Cultures were thoroughly mixed, and the cell density for each competitor was measured at the initial (t = 0) time point by plating 100 μL after two successive 1:1000 dilutions in LB media onto LB + 34 μg/mL chloramphenicol agar plates, supplemented with inducers (100 μM IPTG, 100 nM AHL, and 1 μg/mL aTc). The t = 0 cultures were grown for 24 h at 37 °C shaking at 250 rpm. The final (t = 1) time point cell density was measured at the 24 h time point by the same method as that described for the t = 0 time point. The cell density for each competitor was measured by counting colonies that have distinct colors after imaging under UV light using the ImageJ program. The growth rate for each competitor is calculated by the natural logarithm of the final cell density (t = 1) ratio to the initial cell density (t = 0) that is adjusted for the dilution rate. Relative fitness is then calculated by dividing the growth rate of one competitor relative to the other.

Strain Availability. All strains and sequence info will be made available via AddGene (addgene.org) using the strain IDs in SI Table 3. The sequences for all basic parts are available on the Registry of Standard Biological Parts (partsregistry.org).

■ ASSOCIATED CONTENT

Supporting Information

Additional tables, figures, and movies as described in the text. This information is available free of charge via the Internet at http://pubs.acs.org.

■ AUTHOR INFORMATION

Corresponding Authors

*E-mail: sleight@uw.edu.
*E-mail: hsauro@uw.edu.

Notes

The authors declare no competing financial interest.

■ ACKNOWLEDGMENTS

We thank BEACON: An National Science Foundation Center for the Study of Evolution in Action for funding this research, the Registry of Standard Biological Parts, DNA2.0, the Klavins and Elowitz laboratories for parts, the SBOL Visual V0.0.0 team for part symbols, the 2011 University of Washington iGEM team, Sauro lab (Wilbert Copeland, Bryan Bartley, Kyung Kim, and Michal Galdzicki), and Klavins lab (Rob Egbert) members for useful materials and discussions.

■ REFERENCES

(1) Endy, D. (2005) Foundations for engineering biology. *Nature 438*, 449−453.
(2) Basu, S., Gerchman, Y., Collins, C. H., Arnold, F. H., and Weiss, R. (2005) A synthetic multicellular system for programmed pattern formation. *Nature 434*, 1130−1134.
(3) Levskaya, A., Chevalier, A. A., Tabor, J. J., Simpson, Z. B., Lavery, L. A., Levy, M., Davidson, E. A., Scouras, A., Ellington, A. D., Marcotte, E. M., and Voigt, C. A. (2005) Synthetic biology: Engineering *Escherichia coli* to see light. *Nature 438*, 441−442.
(4) Stricker, J., Cookson, S., Bennett, M. R., Mather, W. H., Tsimring, L. S., and Hasty, J. (2008) A fast, robust, and tunable synthetic gene oscillator. *Nature 456*, 516−519.
(5) Friedland, A. E., Lu, T. K., Wang, X., Shi, D., Church, G., and Collins, J. J. (2009) Synthetic gene networks that count. *Science 324*, 1199−1202.
(6) Gibson, D. G., Glass, J. I., Lartigue, C., Noskov, V. N., Chuang, R. Y., Algire, M. A., Benders, G. A., Montague, M. G., Ma, L., Moodie, M. M., Merryman, C., Vashee, S., Krishnakumar, R., Assad-Garcia, N., Andrews-Pfannkoch, C., Denisova, E. A., Young, L., Qi, Z. Q., Segall-Shapiro, T. H., Calvey, C. H., Parmar, P. P., Hutchison, C. A., Smith, H. O., and Venter, J. C. (2010) Creation of a bacterial cell controlled by a chemically synthesized genome. *Science 329*, 52−56.
(7) Tamsir, A., Tabor, J. J., and Voigt, C. a. (2011) Robust multicellular computing using genetically encoded NOR gates and chemical "wires". *Nature 469*, 212−215.
(8) Mutalik, V. K., Guimaraes, J. C., Cambray, G., Mai, Q.-A., Christoffersen, M. J., Martin, L., Yu, A., Lam, C., Rodriguez, C., Bennett, G., Keasling, J. D., Endy, D., and Arkin, A. P. (2013) Quantitative estimation of activity and quality for collections of functional genetic elements. *Nat. Methods*, 1−12.

(9) Mutalik, V. K., Guimaraes, J. C., Cambray, G., Lam, C., Christoffersen, M. J., Mai, Q.-A., Tran, A. B., Paull, M., Keasling, J. D., Arkin, A. P., and Endy, D. (2013) Precise and reliable gene expression via standard transcription and translation initiation elements. *Nat. Methods*, 1−15.
(10) Ro, D. K., Paradise, E. M., Ouellet, M., Fisher, K. J., Newman, K. L., Ndungu, J. M., Ho, K. A., Eachus, R. A., Ham, T. S., Kirby, J., Chang, M. C., Withers, S. T., Shiba, Y., Sarpong, R., and Keasling, J. D. (2006) Production of the antimalarial drug precursor artemisinic acid in engineered yeast. *Nature 440*, 940−943.
(11) Kern, A., Tilley, E., Hunter, I. S., Legisa, M., and Glieder, A. (2007) Engineering primary metabolic pathways of industrial micro-organisms. *J. Biotechnol. 129*, 6−29.
(12) Nishizaki, T., Tsuge, K., Itaya, M., Doi, N., and Yanagawa, H. (2007) Metabolic engineering of carotenoid biosynthesis in Escherichia coli by ordered gene assembly in *Bacillus subtilis*. *Appl. Environ. Microbiol. 73*, 1355−61.
(13) Tyo, K. E. J., Ajikumar, P. K., and Stephanopoulos, G. (2009) Stabilized gene duplication enables long-term selection-free heterologous pathway expression. *Nat. Biotechnol. 27*, 760−5.
(14) Alper, H., and Stephanopoulos, G. (2009) Engineering for biofuels: exploiting innate microbial capacity or importing biosynthetic potential? *Nat Rev. Microbiol. 7*, 715−23.
(15) Ajikumar, P. K., Xiao, W.-H., Tyo, K. E. J., Wang, Y., Simeon, F., Leonard, E., Mucha, O., Phon, T. H., Pfeifer, B., and Stephanopoulos, G. (2010) Isoprenoid pathway optimization for Taxol precursor overproduction in *Escherichia coli*. *Science (New York, N.Y.) 330*, 70−4.
(16) Peralta-Yahya, P. P., and Keasling, J. D. (2010) Advanced biofuel production in microbes. *Biotechnol. J. 5*, 147−162.
(17) Villalobos, A., Ness, J. E., Gustafsson, C., Minshull, J., and Govindarajan, S. (2006) Gene Designer: A synthetic biology tool for constructing artificial DNA segments. *BMC Bioinformatics 7*, 285.
(18) Chandran, D., Bergmann, F. T., and Sauro, H. M. (2009) TinkerCell: Modular CAD tool for synthetic biology. *J. Biol. Eng. 3*, 19.
(19) Czar, M. J., Cai, Y., and Peccoud, J. (2009) Writing DNA with GenoCAD. *Nucleic Acids Res. 37*, W40−7.
(20) Xia, B., Bhatia, S., Bubenheim, B., Dadgar, M., Densmore, D., and Anderson, J. C. (2011) Developer's and user's guide to Clotho v2.0 A software platform for the creation of synthetic biological systems. *Methods Enzym. 498*, 97−135.
(21) Hillson, N. J., Rosengarten, R. D., and Keasling, J. D. (2012) j5 DNA assembly design automation software. *ACS Synth. Biol. 1*, 14−21.
(22) Bilitchenko, L., Liu, A., and Densmore, D. (2011) The Eugene language for synthetic biology. *Methods Enzym. 498*, 153−72.
(23) Yokobayashi, Y., Weiss, R., and Arnold, F. H. (2002) Directed evolution of a genetic circuit. *Proc. Natl. Acad. Sci. U.S.A. 99*, 16587−91.
(24) Haseltine, E. L., and Arnold, F. H. (2007) Synthetic gene circuits: design with directed evolution. *Ann. Rev. Biophys. Biomol. Struct. 36*, 1−19.
(25) Esvelt, K. M., Carlson, J. C., and Liu, D. R. (2011) A system for the continuous directed evolution of biomolecules. *Nature 472*, 499−503.
(26) Egbert, R. G., and Klavins, E. (2012) Fine-tuning gene networks using simple sequence repeats. *Proc. Natl. Acad. Sci. U.S.A.*, 16817−16822.
(27) Guet, C. C., Elowitz, M. B., Hsing, W., and Leibler, S. (2002) Combinatorial synthesis of genetic networks. *Science 296*, 1466−70.
(28) Cox, R. S., Surette, M. G., and Elowitz, M. B. (2007) Programming gene expression with combinatorial promoters. *Mol. Syst. Biol. 3*, 145.
(29) Sarrion-Perdigones, A., Falconi, E. E., Zandalinas, S. I., Juárez, P., Fernández-del-Carmen, A., Granell, A., and Orzaez, D. (2011) GoldenBraid: An iterative cloning system for standardized assembly of reusable genetic modules. *PloS One 6*, e21622.
(30) Weber, E., Engler, C., Gruetzner, R., Werner, S., and Marillonnet, S. (2011) A Modular Cloning System for Standardized Assembly of Multigene Constructs. *PLoS One 6*, e16765.
(31) Peisajovich, S. G., Garbarino, J. E., Wei, P., and Lim, W. A. (2010) Rapid diversification of cell signaling phenotypes by modular domain recombination. *Science 328*, 368−72.
(32) Lenski, R. E., and Nguyen, T. T. (1988) Stability of recombinant DNA and its effects on fitness. *Trends Ecol. Evol. 3*, S18−20.
(33) Lenski, R. E. (1991) Quantifying fitness and gene stability in microorganisms. *Biotechnology 15*, 173−92.
(34) Dahlberg, C., and Chao, L. (2003) Amelioration of the cost of conjugative plasmid carriage in Eschericha coli K12. *Genetics 165*, 1641−1649.
(35) Dekel, E., and Alon, U. (2005) Optimality and evolutionary tuning of the expression level of a protein. *Nature 436*, 588−592.
(36) Schoustra, S. E., Debets, A. J. M., Slakhorst, M., and Hoekstra, R. F. (2006) Reducing the cost of resistance; experimental evolution in the filamentous fungus *Aspergillus nidulans*. *J. Evol. Biol. 19*, 1115−1127.
(37) Andersson, D. I. (2006) The biological cost of mutational antibiotic resistance: Any practical conclusions? *Curr Opin Microbiol 9*, 461−465.
(38) Bonomo, J., Warnecke, T., Hume, P., Marizcurrena, A., and Gill, R. T. (2006) A comparative study of metabolic engineering anti-metabolite tolerance in *Escherichia coli*. *Metabolic engineering 8*, 227−39.
(39) Eames, M., and Kortemme, T. (2012) Cost−benefit tradeoffs in engineered lac operons. *Science 336*, 911−5.
(40) Maisnier-Patin, S., Berg, O. G., Liljas, L., and Andersson, D. I. (2002) Compensatory adaptation to the deleterious effect of antibiotic resistance in *Salmonella typhimurium*. *Mol. Microbiol. 46*, 355−366.
(41) Babu, M. M., and Aravind, L. (2006) Adaptive evolution by optimizing expression levels in different environments. *Trends Microbiol. 14*, 11−4.
(42) You, L., Cox, R. S., 3rd, Weiss, R., and Arnold, F. H. (2004) Programmed population control by cell−cell communication and regulated killing. *Nature 428*, 868−871.
(43) Balagaddé, F. K., You, L., Hansen, C. L., Arnold, F. H., and Quake, S. R. (2005) Long-term monitoring of bacteria undergoing programmed population control in a microchemostat. *Science (New York, N.Y.) 309*, 137−40.
(44) Canton, B., Labno, A., and Endy, D. (2008) Refinement and standardization of synthetic biological parts and devices. *Nat. Biotechnol. 26*, 787−793.
(45) Sleight, S. C., Bartley, B. A., Lieviant, J. A., and Sauro, H. M. (2010) Designing and engineering evolutionary robust genetic circuits. *J. Biol. Eng. 4*, 12.
(46) Yang, S., Sleight, S. C., and Sauro, H. M. (2013) Rationally designed bidirectional promoter improves the evolutionary stability of synthetic genetic circuits. *Nucleic Acids Res. 41*, e33.
(47) Elena, S. F., and Lenski, R. E. (2003) Evolution experiments with microorganisms: The dynamics and genetic bases of adaptation. *Nat. Rev. Genet. 4*, 457−469.
(48) Sniegowski, P. D., Gerrish, P. J., and Lenski, R. E. (1997) Evolution of high mutation rates in experimental populations of *E. coli*. *Nature 387*, 703−705.
(49) Rose, L. M. R., Simpson, S. C., Tadler, S. C., and E., R. (1991) Long-term experimental evolution in *Escherichia coli*. I. Adaptation and divergence during 2000 generations. *Am. Nat. 138*, 1315−1341.
(50) MacLean, R. C., and Bell, G. (2003) Divergent evolution during an experimental adaptive radiation. *Proc. Biol. Sci. R. Soc. 270*, 1645−50.
(51) Blount, Z. D., Barrick, J. E., Davidson, C. J., and Lenski, R. E. (2012) Genomic analysis of a key innovation in an experimental *Escherichia coli* population. *Nature 489*, 513−8.
(52) Sleight, S. C., Orlic, C., Schneider, D., and Lenski, R. E. (2008) Genetic basis of evolutionary adaptation by *Escherichia coli* to stressful cycles of freezing, thawing, and growth. *Genetics 180*, 431−43.
(53) Meyer, J. R., Dobias, D. T., Weitz, J. S., Barrick, J. E., Quick, R. T., and Lenski, R. E. (2012) Repeatability and contingency in the evolution of a key innovation in phage lambda. *Science 335*, 428−32.

(54) Barrick, J. E., Yu, D. S., Yoon, S. H., Jeong, H., Oh, T. K., Schneider, D., Lenski, R. E., and Kim, J. F. (2009) Genome evolution and adaptation in a long-term experiment with *Escherichia coli*. *Nature 461*, 1243−7.
(55) Cooper, V. S., Schneider, D., Blot, M., and Lenski, R. E. (2001) Mechanisms causing rapid and parallel losses of ribose catabolism in evolving populations of *Escherichia coli* B. *J. Bacteriol. 183*, 2834−2841.
(56) Drake, J. W. (1991) A constant rate of spontaneous mutation in DNA-based microbes. *Proc. Natl. Acad. Sci. U.S.A. 88*, 7160−7164.
(57) Wielgoss, S., Barrick, J. E., Tenaillon, O., Wiser, M. J., Dittmar, W. J., Cruveiller, S., Chane-Woon-Ming, B., Médigue, C., Lenski, R. E., and Schneider, D. (2013) Mutation rate dynamics in a bacterial population reflect tension between adaptation and genetic load. *Proc. Natl. Acad. Sci. U.S.A. 110*, 222−7.
(58) Lovett, S. T. (2004) Encoded errors: Mutations and rearrangements mediated by misalignment at repetitive DNA sequences. *Mol. Microbiol. 52*, 1243−1253.
(59) Gerrish, P. J., and Lenski, R. E. (1998) The fate of competing beneficial mutations in an asexual population. *Genetica 102−103*, 127−44.
(60) Kao, K. C., and Sherlock, G. (2008) Molecular characterization of clonal interference during adaptive evolution in asexual populations of *Saccharomyces cerevisiae*. *Nat. Genet. 40*, 1499−504.
(61) Reyes, L. H., Almario, M. P., Winkler, J., Orozco, M. M., and Kao, K. C. (2012) Visualizing evolution in real time to determine the molecular mechanisms of *n*-butanol tolerance in *Escherichia coli*. *Metab. Eng. 14*, 579−90.
(62) Gerrish, P. J., and Sniegowski, P. D. (2012) Real time forecasting of near-future evolution. *J. R. Soc. Interface 9*, 2268−78.
(63) Gresham, D., Desai, M. M., Tucker, C. M., Jenq, H. T., Pai, D. A., Ward, A., DeSevo, C. G., Botstein, D., and Dunham, M. J. (2008) The repertoire and dynamics of evolutionary adaptations to controlled nutrient-limited environments in yeast. *PLoS Genet. 4*, e1000303.
(64) Reyes, L. H., Winkler, J., and Kao, K. C. (2012) Visualizing evolution in real-time method for strain engineering. *Frontiers Microbiol. 3*, 198.
(65) Winkler, J., and Kao, K. C. (2012) Computational identification of adaptive mutants using the VERT system. *J. Biol. Eng. 6*, 3.
(66) Sleight, S. C., and Sauro, H. M. (2013) Randomized BioBrick assembly: A novel DNA assembly method for randomizing and optimizing genetic circuits and metabolic pathways. *ACS Synth. Biol.*, DOI: 10.1021/sb4000542.
(67) Sleight, S. C., and Sauro, H. M. (2012) Design and construction of a prototype CMY (cyan-magenta-yellow) genetic circuit as a mutational readout device to measure evolutionary stability dynamics and determine design principles for robust synthetic systems. *Artificial Life 13*, 481−488.
(68) Cakar, Z. P., Turanlı-Yıldız, B., Alkım, C., Yılmaz, U., and Nielsen, J. (2012) Evolutionary engineering of Saccharomyces cerevisiae for improved industrially important properties. *FEMS Yeast Res. 12*, 171−82.
(69) Scalcinati, G., Otero, J. M., Vleet, J. R. H., Jeffries, T. W., Olsson, L., and Nielsen, J. (2012) Evolutionary engineering of *Saccharomyces cerevisiae* for efficient aerobic xylose consumption. *FEMS Yeast Res.*, 582−597.